

# The astrophysical signatures of black holes: the horizon, the ISCO, the ergosphere and the light circle

Marek A. Abramowicz

**Abstract** Three advanced instruments planned for a near future (LOFT, GRAVITY, THE EVENT HORIZON TELESCOPE) provide unprecedented angular and time resolutions, which allow to probe regions in the immediate vicinity of black holes. We may soon be able to search for the signatures of the super-strong gravity that is characteristic to black holes: the event horizon, the ergosphere, the innermost stable circular orbit (ISCO), and the photon circle. This review discusses a few fundamental problems concerning these theoretical concepts.

## 1 Introduction

Undoubtedly, the existence of black holes is one of a few most bizarre predictions ever made in the whole acts of physics. The existence of massive objects with gravity strong enough to prevent light from escaping their surfaces was anticipated already in the XVIII century by John Mitchel, and later but independently by Pierre-Simon Laplace. However, the fundamental properties of black holes have been discovered, understood and described in terms of brilliant mathematical developments of Al-

---

Marek A. Abramowicz  
Nicolaus Copernicus Astronomical Center, ul. Bartycka 18, 00-716 Warszawa, Poland; Physics Department, Silesian University (Opava),  
Institute of Astronomy (Prague), The Czech Republic; Professor Emeritus at the Department of Physics, University of Gothenburg, Sweden, e-mail: [marek.abramowicz@physics.gu.se](mailto:marek.abramowicz@physics.gu.se)

bert Einstein’s general theory of relativity, only much later — indeed in our times<sup>1</sup>. Astrophysically, the most important of these fundamental properties are<sup>2</sup>:

1. **Event horizon:** This may be imagined as a sphere (but *not* as a rigid surface) with the “gravitational radius”  $r_G \sim GM/c^2$  surrounding the black hole of the mass  $M$ , from within which nothing may emerge. This is a unique signature of black holes.
2. **Ergosphere:** This is a region around a rotating black hole where spacetime itself is dragged along in the direction of rotation at a speed greater than the local speed of light in relation to the rest of the universe. In this region, negative energy states are possible, which means that the rotational energy of the black hole can be tapped through the “Penrose process”.
3. **Innermost stable circular orbit (ISCO):** This is the smallest circle ( $r = r_{ms}$ ) along which free particles may stably orbit around a black hole. No stable circular motion is possible for  $r < r_{ms}$ . The presence of ISCO in the black hole case is one of the most important features of the black hole accretion [4].
4. **Circular photon orbit:** At a specific radius, often called “the light circle”, photons may circle freely around a black hole.

In the last three decades, robust detections were made of several astrophysical black hole candidates within our Galaxy and in many others galaxies. However, no direct and unambiguous observational signatures of the horizon, the ergosphere, the ISCO and the light circle have been found. The obvious difficulty here is the high angular resolution that is needed to observe the black hole signatures — the “angular size” in the sky of a black hole at a distance  $D$  is  $\delta = r_G/D$ . For SgrA\*, the black hole at the center of our Galaxy, this implies that the smallest observed images of accretion structures around it have a size of a few  $\mu\text{as}$ . At the moment, they cannot be observed, they are too small, but the angular resolution in this range will be reached by advanced new detectors that are planned for the near future.

1. GRAVITY is planned for 2014 by the Max Planck Institute for the Extraterrestrial Physics in Garching, Germany<sup>3</sup>. It is the second-generation VLTI instrument for precision narrow-angle astrometry and interferometric imaging, consisting of four 8m telescopes and a total collecting area of 200 m<sup>2</sup>. It is the only interferometer to allow direct imaging at high sensitivity and high image quality in a large ( $\sim 2''$ ) field of view. It provides precision astrometry with resolution  $\sim 10 \text{ mas}$  (microarcsecond), and imaging with resolution  $\sim 4 \mu\text{as}$  (milliarc-

---

<sup>1</sup> The modern history of black holes started thanks to great discoveries of Schwarzschild [1], Chandrasekhar [2] and Oppenheimer [3], and the follow-up work in the 1960s and the 1970s, done mostly by collaborators and students of Dennis W. Sciama in Cambridge (Carter, Ellis, Gibbons, Hawking, Penrose), John A. Wheeler in Princeton (Bekenstein, Ruffini, Thorne) and Yakov B. Zel’dovich in Moscow (Frolov, Starobinsky) and other researchers (e.g. Israel, Damour, Kerr, Kruksal, Wald).

<sup>2</sup> Here, and in a few other places, I directly quote a Living Review devoted to the subject: Abramowicz & Fragile, *Foundations of Black Hole Accretion Disk Theory*.

<sup>3</sup> Homepage <http://www.mpe.mpg.de/ir/gravity>

second). Note that the apparent size of the gravitational radius of SgrA\*, the Galactic center black hole, is  $10 \mu\text{as}$ .

2. THE EVENT HORIZON TELESCOPE (EHT) The EHT uses the technique of Very Long Baseline Interferometry (VLBI) to synthesize an Earth-sized telescope in order to achieve the highest resolution possible using ground-based instrumentation. Several existing (or planned) radio telescopes are the part of the baseline: ARO/SMT 10m, APEX 12m, ASTE 10m CARMA array of six 10m and nine of 6m antennas, CSO 10m, IRAM 30m, JCMT 15m, SMA array eight 6m antennas. A few more telescopes and arrays will join. The target source is observed simultaneously at all telescopes. The data are recorded at each of the sites and later brought back to a processing facility where they are passed through a special purpose supercomputer. It will be fully operational in 2015.
3. LOFT is a newly proposed space mission selected by ESA as one of the four missions that will compete for a launch opportunity in the 2020s. The Large Area Detector (LAD) on board of LOFT achieves an effective area of  $\sim 10\text{m}^2$  i.e. more than an order of magnitude larger than current spaceborne X-ray detectors in the 2-30 keV range (up to 80 keV in expanded mode). LOFT will have improved energy resolution (better than 260eV) and will be able to investigate range from submillisecond quasi-periodic oscillations(QPOs) to years long transient outbursts. LOFT will provide access (for the first time) to types of information in these signals that are qualitatively new due to the capability to measure dynamical timescale phenomena within their coherence time, where so far only statistical averages of signals were accessible.

It is hoped that data from these new detectors will provide information sufficient to answer several of the questions concerning horizon, ergosphere, ISCO and the light circle that I describe in this review.

## 2 The Kerr metric and its symmetries

The famous Kerr solution [5] describes the spacetime metric of a rotating, uncharged black hole with the total mass  $M$  and the spin  $a = J/Mc$  (here  $J$  is the angular momentum). In the Boyer-Lindquist coordinates the Kerr metric takes the form (in the usual  $c = 1 = G$  units and  $+ - - -$  signature),

$$\begin{aligned}
 g_{\mu\nu}dx^\mu dx^\nu = & \left(1 - \frac{2Mr}{\rho^2}\right) dt^2 + 2\frac{2Mar\sin^2\theta}{\rho^2} dt d\phi \\
 & - \left(r^2 + a^2 + \frac{2Ma^2r\sin^2\theta}{\rho^2}\right) \sin^2\theta d\phi^2 \\
 & - \frac{\rho^2}{\Delta} dr^2 - \rho^2 d\theta^2,
 \end{aligned} \tag{1}$$

where  $\Delta = r^2 - 2Mr + a^2$  and  $\rho^2 = r^2 + a^2 \cos^2 \theta$ .

The Boyer-Lindquist coordinates are most widely used by astrophysicists. They are singular at the horizon, which in this coordinates is given by  $\Delta = 0$ . The Kerr metric is itself not singular at the horizon, which is apparent in the Kerr-Schild coordinates. The Kerr-Schild version of the Kerr metric takes the form,

$$\begin{aligned} g_{\mu\nu} dx^\mu dx^\nu = & \left(1 - \frac{2Mr_*}{\rho_*^2}\right) dt_*^2 - \frac{4Mr_*}{\rho_*^2} dt_* dr_* + \frac{4Mr_*}{\rho_*^2} \sin^2 \theta_* dt_* d\phi_* \\ & - \left(r_*^2 + a^2 + \frac{2Ma^2 r_* \sin^2 \theta_*}{\rho_*^2}\right) \sin^2 \theta_* d\phi_*^2 - \rho_*^2 d\theta_*^2 \\ & - \left(1 + \frac{2Mr_*}{\rho_*^2}\right) dr_*^2 + 2a \sin^2 \theta_* \left(1 + \frac{2Mr_*}{\rho_*^2}\right) dr_* d\phi_*, \end{aligned} \quad (2)$$

where  $\rho_*^2 = r_*^2 + a^2 \cos^2 \theta_*$ .

The Kerr metric in the Boyer-Lindquist coordinates does not depend on  $t, \phi$ . In the Kerr-Schild coordinates it does not depend on  $t_*, \phi_*$ . This is a sign of the Killing symmetries. The Killing vectors defined by (in the Boyer-Lindquist coordinates)

$$\eta^\mu = \delta_t^\mu, \quad \xi^\mu = \delta_\phi^\mu \quad (3)$$

obey the Killing equation and commute,

$$\nabla_\nu \eta_\mu + \nabla_\mu \eta_\nu = 0, \quad \nabla_\nu \xi_\mu + \nabla_\mu \xi_\nu = 0, \quad (4)$$

$$\xi^\nu \nabla_\nu \eta_\mu = \eta^\nu \nabla_\nu \xi_\mu. \quad (5)$$

For commuting Killing vectors one may write convenient relations,

$$\begin{aligned} \xi^\nu \nabla_\nu \eta_\mu &= \eta^\nu \nabla_\nu \xi_\mu = -\frac{1}{2} \nabla_\nu (\xi^\mu \eta_\mu), \\ \eta^\nu \nabla_\nu \eta_\mu &= -\frac{1}{2} \nabla_\nu (\eta^\mu \eta_\mu), \\ \xi^\nu \nabla_\nu \xi_\mu &= -\frac{1}{2} \nabla_\nu (\xi^\mu \xi_\mu), \end{aligned} \quad (6)$$

which often allow to keep Christoffels symbols out of calculations<sup>4</sup>.

The existence of the Killing vectors  $\eta^\mu, \xi^\mu$ , implies conservation of energy  $\mathcal{E}$  and angular momentum  $\mathcal{L}$  in geodesic motion,

$$\{u^\mu \nabla_\mu u_\nu = 0\} \Rightarrow \left\{ \begin{array}{l} u^\mu \nabla_\mu \mathcal{E} = 0 \text{ for } \mathcal{E} \equiv \eta^\mu u_\mu \\ u^\mu \nabla_\mu \mathcal{L} = 0 \text{ for } \mathcal{L} \equiv -\xi^\mu u_\mu \end{array} \right\} \quad (7)$$

<sup>4</sup> At <http://www.physics.uci.edu/~etolleru/KerrOrbitProject.pdf> the Christoffel symbols are given (by Tollerud, 2007) in the form of a `Mathematica` package. Unfortunately, there is an error in the Kerr metric: the  $g_{t\phi}$  metric component is (consistently everywhere) factor of 2 too big. See also [6]

The specific angular momentum  $\ell \equiv \mathcal{L}/\mathcal{E}$  is obviously also a constant of geodesic motion. In a general, not necessarily geodesic case, the *circular* orbits are given by  $u^\mu = A(\eta^\mu + \Omega \xi^\mu)$ , where  $\Omega$  is the angular velocity, connected to the specific angular momentum by,

$$\ell = (\Omega - \omega) \frac{\tilde{r}^2}{1 + \Omega \omega \tilde{r}^2}, \quad (8)$$

$$\omega = -\frac{\xi^\mu \eta_\mu}{\xi^\nu \xi_\nu} = (\text{frame dragging}), \quad (9)$$

$$\tilde{r}^2 = -\frac{\xi^\nu \xi_\nu}{\eta^\mu \eta_\mu} = (\text{gyration radius})^2. \quad (10)$$

From (3) it follows that in the Boyer-Lindquist coordinates these quantities are expressed by,

$$\mathcal{E} = u_t, \quad \mathcal{L} = -u_\phi, \quad \ell = -\frac{u_\phi}{u_t}, \quad \Omega = \frac{u^\phi}{u^t} = \frac{d\phi}{dt}. \quad (11)$$

### 3 The Horizon

A coordinate independent condition for the Kerr black hole horizon could be expressed by

$$(\eta^\nu \xi_\nu)^2 - (\eta^\nu \eta_\nu)(\xi^\mu \xi_\mu) = 0. \quad (12)$$

A presence of the horizon is most often argued from observational estimates of the ‘‘compactness parameter’’  $\xi \sim R_G/R$ . Here  $R$  is the measured size of the black hole candidate, and the gravitational radius  $R_G$  is known from a mass measurement. Mass measurements are *very* accurate in a few cases (based on Kepler’s laws and precise orbit measurements), but in most cases they are not accurate (orbits are unobserved directly). Size measurements are not yet accurate, and in addition the measured size is only an upper limit. In most of the considered cases, one estimates not the size of the horizon, but the size of ISCO or the size of the light circle radius.

Narayan [10, 11, 9] presented arguments that point to the horizon presence more directly. When a central object accretes matter through an accretion disk, a part of its radiation,  $L_{disk}$ , originates at the disk, and a part  $L_{surf}$  at the surface of the object. The surface may radiate itself, or reflect (re-radiate) a part of the disk radiation. The total is therefore  $L = L_{disk} + L_{surf}$ . The horizon of the black hole cannot radiate or reflect  $L_{surf} = 0$ , and therefore in the black hole case,  $L = L_{disk}$ . Thus, black holes should look dimmer than non-black-hole objects with the similar accretion disks.

This indeed is observed in the case of accreting neutron stars vs. accreting black holes, in the galactic X-ray binaries, as explained in Figure 1. In the figure luminosities of the binary black hole sources are compared with luminosities of the binary neutron star sources with the same orbital binary period. In these binaries, the compact object (a black hole or a neutron star) has a close companion, which is a low

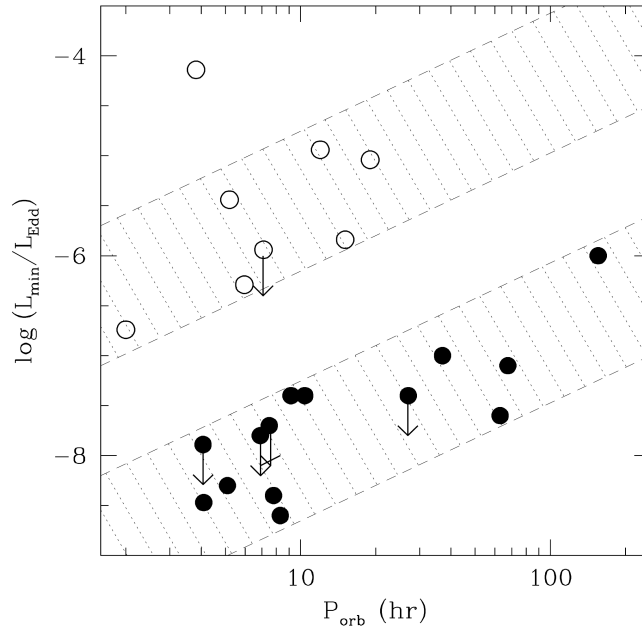


**Fig. 1** Eddington-scaled luminosities (0.5–10 keV) of BH transients (filled circles) and NS transients (open circles) versus the orbital period (see [7]; [8]). Only the lowest quiescent detections or Chandra/XMM upper limits are shown. The plot shows all systems with known orbital periods, which have optical counterparts and good distance estimates. The diagonal hatched areas delineate the regions occupied by the two classes of sources and indicate the observed dependence of luminosity on orbital period. Note that the BH systems are on average nearly 3 orders of magnitude fainter than the NS systems with similar orbital periods. Figure and caption from [9].

mass “normal” star. The companion loses mass which is accreted onto the compact object via the accretion disk. The luminosity of the accretion disk depends on the accretion rate, which is determined by the mass loss rate from the companion. The accretion rate cannot be directly measured, but the precisely and directly observed orbital period is a rather accurate indicator of the accretion rate — sources with the same orbital periods should have the same accretion rates. In figure 1, luminosities are given in terms of the Eddington luminosity,  $L_{\text{Edd}} = 10^{38} M/M_{\odot}$  [erg/s] which is proportional to the mass of the compact object  $M$ . One should note that the neutron star sources are order of magnitudes more luminous than the black hole sources in binaries with the same binary periods. This difference may be indeed due to the (already mentioned) fact that in the neutron star sources, matter that arrives at the surface may emit radiation, while in the black hole sources matter is lost without a trace inside the black hole. However, it was pointed out by several authors, e.g. [12, 13], for various reasons, rigid surfaces of *strange stars* may also absorb all matter without a trace.

Narayan's argument based on the evidence of some radiation lost inside the black hole works, in a different version, also for the super-massive black holes, in particular for SgrA\*, the accreting black hole in the center of our Galaxy, for which the mass,  $M = 4 \times 10^6 M_\odot$ , was accurately measured from the analysis of stellar orbits in its vicinity. The accreting black hole has a very low luminosity. As figure 2 explains, a hypothesis that SgrA\* is a dark object with a rigid surface is inconsistent with observations and the standard accretion theory of radiatively inefficient accretion flows (RIAF).

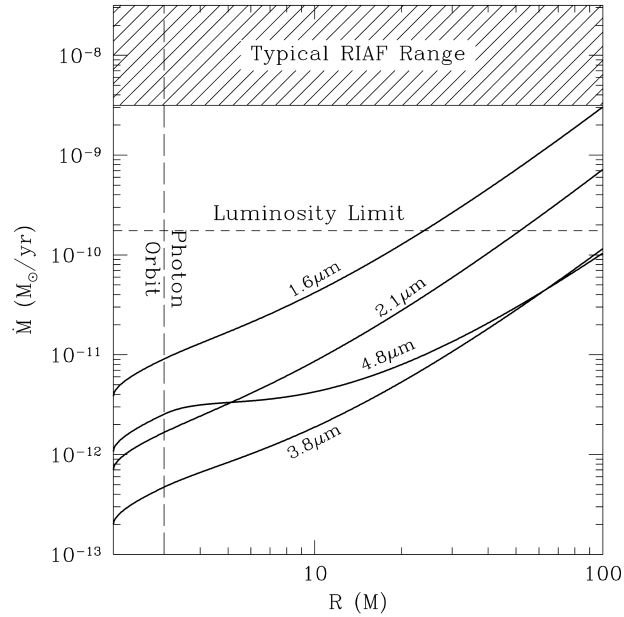


**Fig. 2** The four solid lines show independent upper limits on the mass accretion rate at the surface of Sgr A\* (assuming the source has a surface) as a function of the surface radius  $R$ . Each limiting curve is derived from a limit on the quiescent flux of Sgr A\* in an infrared band. The hatched area at the top labeled “Typical RIAF Range” corresponds to the mass accretion rate in typical ADAF models of Sgr A\* (e.g. [14]). The horizontal dashed line represents the minimum accretion rate needed to power the bolometric luminosity of Sgr A\*. Figure and caption from [9], after [15].

## 4 The Ergosphere

<sup>5</sup> The surface of ergosphere in Kerr geometry is given by the covariant condition,

$$\eta^\mu \eta_\mu = 0. \quad (13)$$

In the Boyer-Lindquist coordinates this is equivalent to  $g_{tt} = 0$ . Thus, inside the ergosphere, the Killing vector  $\eta^\mu$  is spacelike, and therefore it is possible that, for a timelike four-velocity  $u^\mu$  of a free particle, the conserved energy is negative,

$$u^\mu \eta_\mu = \mathcal{E} < 0. \quad (14)$$

### 4.1 The Penrose proces

Penrose [16] considered<sup>6</sup> a free falling particle with energy  $\mathcal{E}_{\text{in}}$ , which enters the ergosphere of a rotating black hole. He imagined that the particle disintegrates there into two particles, with energies  $\mathcal{E}_{(-)} < 0$  and  $\mathcal{E}_{(+)} > 0$ . Then, the particle with negative energy  $\mathcal{E}_{(-)}$  falls into the black hole, and the other one escapes to infinity with positive energy,  $\mathcal{E}_{\text{out}} = \mathcal{E}_{(+)}$ . Since energy conservation implies that  $\mathcal{E}_{(-)} + \mathcal{E}_{(+)} = \mathcal{E}_{\text{in}}$ , one deduces that  $\mathcal{E}_{\text{out}} > \mathcal{E}_{\text{in}}$ , so there is a gain of energy “at infinity”. The negative energy particle absorbed by the black hole has also a negative angular momentum,  $\mathcal{L}_{(-)} < 0$ . The source for the gain of energy at infinity is therefore the rotational energy of the black hole.

Soon after Penrose’s discovery that rotating black holes may be energy sources, several authors suggested that the Penrose process may power relativistic jets observed in quasars (and later in microquasars). However, a careful analysis by [18, 19, 20, 21, 22] and others, shown that it is unlikely that negative energy states, necessary for the Penrose process to work, may be achieved through the particles disintegration inside ergosphere. The same conclusion was reached more recently by [23] for high-energy collision of particles. The reason is that in the case of disintegration, for a negative energy state to occur velocities of fragments measured in their center of mass frame should be very relativistic,  $v > c/2$ . In the case of collisions, the particles with positive energies cannot escape, as they must have large and negative radial momenta. Thus, they are captured (together with the negative energy particles) by the black hole.

In the context of the super-energetic collisions there is a disagreement between two opinions, based on recently obtained results. Firstly, Silk and his collaborators [24] claimed that in the center-of-mass frame, the energy of particular types of collisions may be arbitrary large and that this may lead to astrophysically important

<sup>5</sup> In this Section I quote extensively from a paper in preparation: Abramowicz, Gourgoulhon, Lasota, Narayan & Tchekhovskoy (2013), *Blandford-Znajek mechanism as the Penrose process. Application to Magnetically Arrested Disks*

<sup>6</sup> See also [17]

and interesting consequences. Secondly, Bejger and collaborators [23] claimed that consequences of such collisions are unobservable. Both results have been published and attracted a considerable attention. There is a vigorous follow-up going on — see [25] for the most recent significant result, which confirms and expands results obtained by [23]: *black holes are neither particle accelerators nor dark matter probes*. This leaves magnetic processes as the only astrophysically realistic way to extract rotational energy from a rotating black hole.

## 4.2 The Blandford-Znajek Mechanism

The presence of ergosphere is today discussed mostly in two contexts: the origin of relativistic jets and super-energetic collisions of particles deep inside the ergosphere.

In the jet context, Tchekhovskoy, Narayan and their collaborators [26, 27, 28] have found that the famous Blandford-Znajek mechanism [29] works for “magnetically arrested disks”, i.e. a special type of magnetized black hole accretion [30]. There are several issues here that need to be studied and explained.

## 5 The ISCO

The existence of ISCO is probably the single most important strong-gravity effect in the whole black hole accretion disk theory. There is, however, a controversy concerning the ISCO. According to one view [31, 32], for small accretion rates, location of ISCO determines the “inner edge” of the disk which separates the part of the disk where matter rotates on almost Keplerian, almost circular orbits, from the plunging-in region, where matter falls in into the black hole almost freely. There is no (significant) radiation coming from the plunging-in region, and stresses there are negligible. Numerous well-known and widely used results in accretion theory depend on the assumption that ISCO is the sharp boundary between the two different accretion regimes. In particular, works on the black hole spin estimate based on spectral fitting adopt this assumption [33, 34]. According to the opposite view [35], most recently eloquently summarized by Balbus [36], ISCO is not an important feature of black hole accretion even for small accretion rates, because the magnetohydrodynamical MRI instability makes the flow unstable and turbulent on both sides of ISCO.

It is obvious that because the ISCO appears as an important ingredient in numerous specific (and important) results of the black hole accretion disk theory, it is one of its few pillars on which the theory rests. For all these reasons, the ISCO receives more attention in my review than the other three black hole accretion disk signatures (horizon, ergosphere, circular photon orbit).

### 5.1 ISCO for Keplerian, circular orbits (circular geodesics)

In this Section we use the Boyer-Lindquist coordinates (1). Let us consider a test particle with mass  $m$  which moves on the equatorial plane,  $\theta = \pi/2$ . For such a motion, the polar components of the four velocity vanish,  $u^\theta = 0 = u_\theta$ , and from  $u_\mu u_\nu g^{\mu\nu} = 1$  it follows that,

$$(u_t)^2 g^{tt} + 2u_t u_\phi g^{t\phi} + (u_\phi)^2 g^{\phi\phi} + (u^r)^2 g_{rr} = 1. \quad (15)$$

Let us now assume that the motion is almost circular in the sense that  $r(s) = r_0 + \delta r(s)$  and  $|\delta r(s)| \ll r_0$  for some constant positive  $r_0$ , which corresponds to the radius of the circle in the Boyer-Lindquist coordinates ( $s$  is the spacetime length along the trajectory). Using the Boyer-Lindquist expressions (11) for the conserved energy  $\mathcal{E}$  and the conserved specific angular momentum  $\ell$ , one may write equation (15) as,

$$\frac{1}{2}|g_{rr}|(\delta\dot{r})^2 = E - \mathcal{U}_{\text{eff}}(r, \ell), \quad (\delta\dot{r}) \equiv \frac{d(\delta r)}{ds}, \quad (16)$$

$$\mathcal{U}_{\text{eff}} = -\frac{1}{2} \ln [g^{tt} - 2\ell g^{t\phi} + \ell^2 g^{\phi\phi}], \quad (17)$$

where  $E = \ln \mathcal{E}$  may also be rightly called the energy because in the Newtonian limit it is  $E \rightarrow E_{\text{Newton}}$ , and  $\mathcal{E} \rightarrow E_{\text{Newton}} + 1$ . The effective potential  $\mathcal{U}_{\text{eff}}(r, \ell)$  equals its Newtonian counterpart in the Newtonian limit. Except of  $|g_{rr}| \rightarrow 1$ , equation (16) has its form identical with the corresponding Newtonian one, very familiar from the classical Mechanics. Thus, using the same procedure as in the Newtonian case, one may derive equations that govern the strictly circular geodesic motion  $\delta\dot{r} = 0$ , and a slightly perturbed  $\delta\dot{r} \neq 0$  one,

$$\left( \frac{\partial \mathcal{U}_{\text{eff}}}{\partial r} \right)_\ell = 0 \Rightarrow \partial_r g^{tt} - 2\ell \partial_r g^{t\phi} + \ell^2 \partial_r g^{\phi\phi} = 0, \quad (18)$$

$$\frac{1}{|g_{rr}|} \left( \frac{\partial^2 \mathcal{U}_{\text{eff}}}{\partial r^2} \right)_\ell = \kappa^2 \quad \text{and} \quad \boxed{\delta\ddot{r} + \kappa^2 \delta r = 0}. \quad (19)$$

As the Kerr metric components  $g^{\mu\nu} = g^{\mu\nu}(r)$  are known functions of the Boyer-Lindquist coordinate  $r$  on the equatorial plane, the quadratic equation in (18) may be easily solved. Its solution  $\ell = \ell_K(r)$  represents the Keplerian angular momentum distribution,

$$\ell_K = \frac{M^{1/2}(r^2 - 2aM^{1/2}r^{1/2} + a^2)}{r^{3/2} - 2Mr^{1/2} + aM^{1/2}}, \quad (20)$$

$$(\Omega_K)^2 = \frac{GM}{(r^{3/2} + aM^{1/2})^2}, \quad (21)$$

$$\omega_r = \frac{\kappa}{A} = \Omega_K \left( 1 - 6x^{-1} + 8a_* x^{-3/2} - 3a_*^2 x^{-2} \right)^{1/2}. \quad (22)$$

Here  $a_* = a/M$ . In the second line (21) we give the Keplerian angular velocity  $\Omega_K$ , and in the third line (22) the the radial epicyclic frequency, which is the redshifted eigenvalue  $\kappa$ . In the Boyer-Lindquist coordinates the redshift factor is  $A = u^t$ , and covariantly,

$$A = \frac{1}{[(\eta^\mu \eta_\mu) + 2\Omega(\xi^\mu \eta_\mu) + \Omega^2(\xi^\mu \xi_\mu)]^{1/2}}. \quad (23)$$

From the simple harmonic oscillator equation in (19) it follows that for  $\kappa^2 < 0$  the circular Keplerian orbits are unstable. The Innermost Stable Circular Orbit (ISCO) is located therefore at the radius  $r_{ms}$  defined by equation  $\kappa^2(r_{ms}) = 0$ . Its solution yields,

$$\begin{aligned} \text{ISCO location : } r_{ms} &= M \left\{ 3 + Z_2 - [(3 - Z_1)(3 + Z_1 + 2Z_2)]^{1/2} \right\}, \\ Z_1 &= 1 + (1 - a_*^2)^{1/3} [(1 + a_*)^{1/3} + (1 - a_*)^{1/3}], \\ Z_2 &= (3a_*^2 + Z_1^2)^{1/2}. \end{aligned} \quad (24)$$

The location of ISCO for different Kerr black hole spins,  $r_{ms}(a)$ , is shown in Figure 3, together with locations of other characteristic radii (in terms of the Boyer-Lindquist coordinate  $r$ ),

$$\text{photon } r_{\text{ph}} = 2M \left\{ 1 + \cos \left[ \frac{2}{3} \cos^{-1}(a_*) \right] \right\}, \quad (25)$$

$$\text{bound } r_{\text{mb}} = 2M \left( 1 - \frac{a_*}{2} + \sqrt{1 - a_*} \right), \quad (26)$$

$$\text{horizon } r_{\text{H}} = M \left( 1 + \sqrt{1 - a_*^2} \right), \quad (27)$$

$$\text{ergosphere } r_0 = M \left( 1 + \sqrt{1 - a_*^2 \cos^2 \theta} \right). \quad (28)$$

## 5.2 The Shakura-Sunyaev ISCO paradigm for thin accretion disks

<sup>7</sup> Many basic results of the black hole accretion theory are a direct consequence of the existence of the ISCO. They are reviewed and discussed e.g. in [4]. The “standard” black hole stationary, non-magnetized, accretion disks are characterized by small (very sub-Eddington) accretion rates,  $\dot{M} \ll \dot{M}_{\text{Edd}}$ , and small vertical thickness,  $h \equiv H/r \ll 1$ . Their mathematical model was developed (in Newton’s theory) by Shakura and Sunyaev in the most influential and important paper in the accretion

---

<sup>7</sup> In this Section I quote *in extenso* a few paragraphs from an unfinished draft of an unpublished paper by Abramowicz, Horák & Kluźniak, *The MRI in the plunge-in region: the Shakura-Sunyaev ISCO paradigm confirmed*, 2013, in preparation.

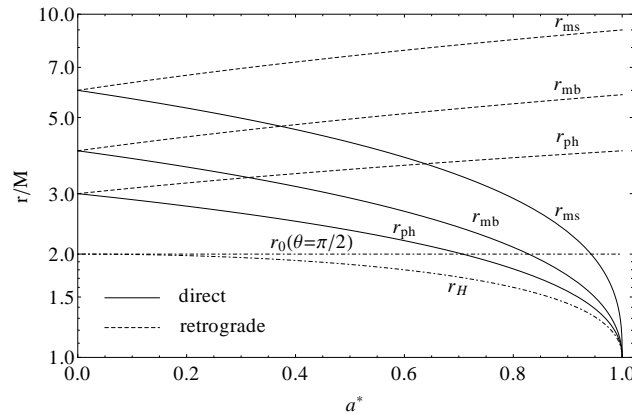


**Fig. 3** The location of ISCO for different Kerr black hole spins,  $r_{ms}(a)$  together with locations of other characteristic radii (in terms of the Boyer-Lindquist coordinate  $r$ ). See text.

disk theory [37], hereafter SS73. Its general relativistic version, proper for the Kerr black holes, was found by Novikov and Thorne [38], hereafter NT73.

For such disks, the ISCO behaves like a physical boundary, separating the *disk proper* from the *plunging* region. In the disk proper (we will call it simply “disk”), i.e. in the region  $r > r_{ms}$ , matter moves on nearly circular, nearly Keplerian orbits. Consequently, the angular momentum of the disk is nearly Keplerian,  $\ell(r) \approx \ell_K(r)$ . Dissipation of orbital energy and angular momentum is significant, and most ( $\sim 98\%$ ) of the accretion flow radiation comes from there. In the plunging region,  $r < r_{ms}$ , matters nearly free falls. Stresses are ineffective in dissipating energy and transporting angular momentum. Consequently, very little radiation ( $\sim 2\%$ ) comes from this region, and the angular momentum distribution there is almost constant,  $\ell(r) \approx \text{const}$ .

The SS73 and NT73 models were developed two decades before Balbus and Hawley [39] made the seminal discovery that the torque needed for accretion discs to operate originates from the turbulence caused by the Magneto Rotational Instability (MRI) which weakly magnetized, differentially rotating fluids suffer. The view that the MRI is crucial in providing that necessary torque, was supported by numerous follow-up works, mostly based on magnetohydrodynamical numerical simulations. Today it is generally accepted by a vast majority of the black hole accretion disk researchers<sup>8</sup>. For the review of successes of the hypothesis of the MRI induced torque, see [42] and [43].

With no knowledge of the true nature of viscous torques in accretion disks, the SS73 and NT73 models adopted a heuristic viscosity prescription based on the assumption that the torque is proportional to the total pressure,

<sup>8</sup> However, [40], [41] and others pointed to some difficulties with the MRI concept and also with its description in the shearing box simulations.

$$\mathcal{T} = \alpha p, \quad (29)$$

with  $0 < \alpha < 1$  being a parameter. The SS73 and NT73 models have also adopted other simplifying assumptions, among them that at the ISCO the torque is zero,

$$\mathcal{T}(r_{\text{ms}}) = 0, \quad (30)$$

and that there is no radial (advective) heat transport in the disk. These assumptions introduced an artificial singularity at the ISCO, not relevant for calculating spectra, but obviously calling for a more accurate treatment of the flow near ISCO. This more accurate treatment was initiated in works by [44] and [45]. It eventually matured as the *slim disk* model [46].

Slim disks assume the alpha-viscosity prescription (29), but do *not* assume the zero-torque condition at ISCO (30). Instead, they consistently solve (numerically) the full set of the (relativistic, in the Kerr geometry) Navier-Stokes equations,  $\nabla_{\mu} T_{\mu}^{\nu} = 0$ , expanded in terms of the small vertical disk thickness  $h$ , up to the quadratic order  $\mathcal{O}(h^2)$ . This includes solving the vertical radiative transfer in the diffusion approximation [47]. Mathematically, the slim disk equations form an eigen-value problem, with the eigen-value being the angular momentum of matter crossing the black hole horizon. The physical reason for the eigen-value nature of the problem is that the black hole accretion must necessarily be transonic, with the sonic point  $r_S$  being the critical (saddle) point of the slim disk differential equations. The regularity conditions at  $r_S$  assure that its location is very close to ISCO,  $r_S = r_{\text{ms}} - A^2 h^2$ , where  $A$  depends on the equation of state, with the the sound speed  $C_S \ll c$ , which is always true for very thin disks,  $h \ll 1$  [48].

The slim disk calculations fully confirmed that, for  $\dot{M} \ll \dot{M}_{\text{edd}}$  and  $h \ll 1$ , the ISCO was a (quite sharp) boundary between disk and plunging region, and that the stress at ISCO was indeed small. Despite that, the ISCO paradigm was challenged mostly by Krolik [35], but also by others, on the ground that the alpha viscosity prescription (29) used in the slim disk calculations was not adequate, because (according to their view) it cannot properly describe the MRI torque accross the ISCO. [31] and [32] argued that *independently on the physical nature of the torque*, for the thin ( $h \ll 1$ ) disks the small stress at ISCO is a consequence of the angular momentum conservation. However, Paczyński's clear arguments have not been accepted (or understood) by a few opponents of the standard ISCO paradigm. It was obvious that the opponents could be convinced only by calculations or arguments that specifically include the MRI induced turbulence.

Fortunately for the validity of the standard ISCO paradigm, such calculations and arguments are now available. Firstly, [49] convincingly demonstrated in terms of MHD shear box simulations (which included vertical stratification and radiative cooling) that the standard Shakura-Sunyaev viscosity prescription (29) adequately describes the MRI torque (see also [50]). Secondly, [51], [52] and [53] performed recently MHD global simulations of the black hole accretion disks, concluding that for geometrically thin accretion disks used in their simulations (i.e. with  $h \sim 0.05 - 0.1$ ):

1. The angular momentum distribution in the flow is characterized by  $\ell(r) \sim \ell_K(r)$  outside ISCO (i.e. for  $r > r_{ms}$ ) and  $\ell(r) \sim \text{const}$  inside ISCO (i.e. for  $r < r_{ms}$ ), see Figure 4. Correspondingly to this (as  $\delta E \sim \Omega \delta \ell$ ), there is very small energy dissipation inside ISCO, and therefore very little radiation may originate there.
2. Turbulent activity is pronounced at radii beyond about  $10r_G$ . Flow is nearly laminar inside the ISCO, see Figure 4. This agrees with  $\ell(r) \sim \text{const}$  there, and also suggests that the bulk of the dissipation occurs in the disk outside the ISCO, but *not* in the plunging region.

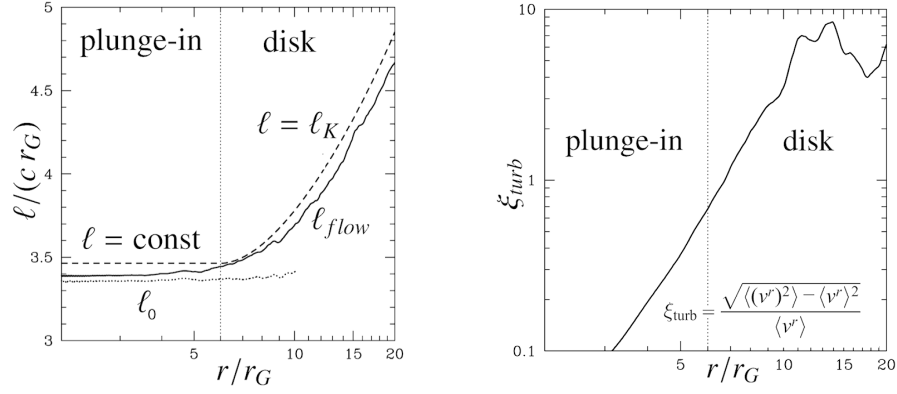


**Fig. 4 Left:** Recent three-dimensional MHD simulations by [51], [52] and [53] proved that the angular momentum distribution,  $\ell_{flow}$ , in the vertically thin accretion flow ( $h < 0.1$ ) agrees within  $\sim 2\%$  with that predicted by the standard ISCO paradigm in SS73, NT73 and the slim disk models, i.e. that  $\ell = \ell_K$  in the “disk” region outside ISCO, and  $\ell = \text{const}$  in the “plunge-in” region inside ISCO. The vertical dotted line indicates the ISCO. The horizontal dotted line corresponds to the *total* angular momentum transport, divided by accretion rate,  $\ell_0 = \dot{J}/\dot{M}$ . Its constancy over the large range of radii proves that the steady state has been achieved in the simulations. Figure adopted from [51]. **Right:** Time averaged profile of  $\xi_{turb}$ , which measures the relative magnitude of turbulent fluctuations in the accreting gas. The fluid becomes mostly laminar inside the ISCO. Figure taken from [51].

The above mentioned new results could be taken as the final proof of the validity of the standard ISCO paradigm if not one remaining subtle point. Most of the present understanding of the properties of MIR is based on the MHD shear box simulations, that are usually done with two particular assumptions — that the radial component of the flow is negligible, and that the radial profile of angular momentum corresponds to the Newtonian Keplerian one,

$$V_r = 0, \quad (31)$$

$$\ell(r) \sim r^s, \quad \text{with } s = 1/2. \quad (32)$$

In the disk proper these conditions are satisfied. However, in the plunging region they are *not* fulfilled. Instead of  $V_r = 0$  one has  $V_r \gg C_S$  (indeed  $V_r \sim c$ ), and in-

stead of  $s = 1/2$  one has  $s = 0$ . These differences could *very* significantly affect the strength of the MRI, as argued by [54].

However, works on slim disks and MHD simulations that support the standard ISCO paradigm have adopted assumption (directly or not) that the MRI induced torque is not qualitatively different on both sides of ISCO. For example, in terms of the alpha prescription this corresponds to  $\alpha(r) \approx \text{const}$ <sup>9</sup>.

If one could argue that the MRI properties on both sides of ISCO are indeed qualitatively the same (despite the differences in the behavior of  $V_r$  and  $s$ ), then the validity of the ISCO paradigm would be finally proven.

Most recently such arguments have been put forward by [36], who stated in the Abstract of his paper that: *the defining properties of the MRI — its maximum growth rate and the direction of the associated eigenvector displacement — remain unchanged as the Rayleigh discriminant passes from positive to negative values*. In other words, because the “Rayleigh discriminant” is simply  $\kappa^2$ , i.e. the square of the radial epicyclic frequency which changes its sign at the ISCO, *the properties of MRI are the same on both sides of the ISCO*. Thus, if the arguments in [36] are correct, they provide the last missing point to complete the proof of the validity of the standard ISCO paradigm.

### 5.3 Leaving the ISCO

Abramowicz et al. [4] revisited Krolik and Hawley’s [56] discussion of the location of the “inner edge”  $r_{in}$  of accretion disks around black holes, and expanded it to include disks with around Eddington accretion rates. The concept of the inner edge may be introduced by several empirical definitions of the accretion disk inner edge, each serving a different practical purpose:

1. **The potential spout edge**  $r_{in} = r_{pot}$ , where the effective potential  $\mathcal{U}_{\text{eff}}$ , see equation (17) forms a self-crossing Roche lobe, and accretion is governed by the Roche lobe overflow.
2. **The sonic edge**  $r_{in} = r_{son}$ , where the transition from subsonic to transonic accretion occurs. Hydrodynamical disturbances do not propagate upstream a supersonic flow, and therefore the subsonic part of the flow is “causally” disconnected from the supersonic part.
3. **The variability edge**  $r_{in} = r_{var}$ , the smallest radius where orbital motion of coherent spots may produce quasi periodic variability.
4. **The stress edge**  $r_{in} = r_{str}$ , the outermost radius where the Reynolds stress is small, and plunging matter has no dynamical contact with the outer accretion flow;
5. **The radiation edge**  $r_{in} = r_{rad}$ , the innermost place from which significant luminosity emerges.

---

<sup>9</sup> But see [55]

6. **The reflection edge**  $r_{in} = r_{ref}$ , the smallest radius capable of producing significant fluorescent iron line.

They found [4] that: “for black hole accretion disks with very sub-Eddington luminosities all these inner edges locate at ISCO. Thus, in this case, one may rightly consider ISCO as the unique inner edge of the black hole accretion disk. However, even for moderately higher luminosities, there is no such unique inner edge as differently defined edges locate at different places. Several of them are significantly closer to the black hole than ISCO. The differences grow with the increasing luminosity. For nearly Eddington luminosities, they are so huge that the notion of the inner edge losses all practical significance.”

#### 5.4 Evidence for ISCO from the observed variability (QPOs)

Quasi periodic oscillations (called QPOs) are high frequency (about kHz) oscillations in the X-ray fluxes from neutron star and black hole sources in the Galactic X-ray sources (they have been also observed in a few extra-Galactic sources and in SgrA\*). In many sources they appear as a pair of oscillations, and are called the “twin-peak” QPOs. Before 2000, twin peak kHz QPOs have been observed only in the neutron star sources. It was believed that they must be connected to the neutron star rigid surfaces, and cannot occur in the black hole sources. Kluźniak & Abramowicz suggested (see [57]) that the twin peak kHz QPOs are due to a non-linear resonance in accretion disks oscillations, and for this reason their frequencies should have ratios close to those of small natural numbers, for example 3:2. Their prediction that the twin peak QPOs should also appear in the BH sources was soon confirmed by Strohmayer [58], who observed a twin peak QPOs in the BH candidate GRO J1655-40. The 3:2 non-linear resonance explanation is now generally accepted, but despite its successes in finding general signatures of the resonance in the observational data, several questions remain unanswered, in particular the behavior of the quality factor  $Q$  of the QPOs. Barret, Kluźniak et al. (see [59]) found that  $Q$  of the lower-frequency QPO in the neutron-star sources increase with increasing QPO frequency up to  $Q \gg 200$  and then it drops. The high-frequency QPO has  $Q \sim 10$  and does not follow the same pattern. There is a consensus that this rules out any kinematical model of QPOs as orbiting clumps or spots. The drop in  $Q$  of the lower-frequency QPO is attributed to the existence of the ISCO (see Figure 5), but this interpretation is not generally accepted.

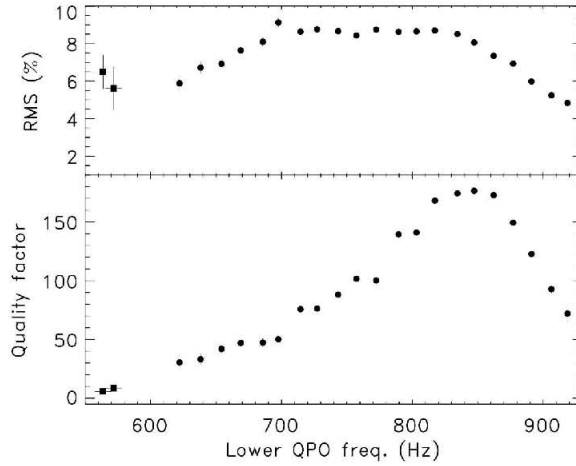


**Fig. 5** A sudden drop in the quality factor  $Q$  of the observed twin peak QPO (lower frequency) was suggested as an evidence for the existence of the ISCO. The data presented here is from the Rossi X-ray Timing Explorer satellite observations of the neutron star binary source 4U 1636-536. The source shows quasi-periodic oscillations with *varying* frequencies in the range 650 Hz–900 Hz. The sharp drop in the quality factor (bottom panel) was recorded at the frequency  $\sim 870$  Hz. Figure from [60].

## 6 The Light Circle

<sup>10</sup> The light circle issue is an emerging topic [61] that is connected to improving observational potentials in the sub-millarcsecond radio imaging of the black hole sources, in particular SgrA\*, i.e. the black hole in the center of our Galaxy.

The shortest timescale that may be in principle observed in the accreting black hole sources is not connected to the accretion flow, but to the strong gravity itself which close to the horizon loops photon trajectories around the black hole (see Figure 6). Signals from some transient events in accretion disk, e.g., random short-lived flares, may therefore reach the observer repeatedly with delays corresponding to the travel time around the circular photon orbit. The looped signals will introduce a correlation in the variability data, with the timescale  $T_{\text{photon}}$  shorter than the timescale at ICSSO,  $T_{\text{ISCO}}$ . For a non-rotating black hole it is,

$$T_{\text{photon}} = 32.6M, \quad T_{\text{ISCO}} = 92.3M. \quad (33)$$

If the conditions are right, signal from some transient events in accretion disk, e.g., random short-lived flares, may reach the observer repeatedly with delays corre-

<sup>10</sup> Based on a lecture by M. Bursa given at the 9 RAGtime Workshop in Opava, 19-21 September, 2007 [61].

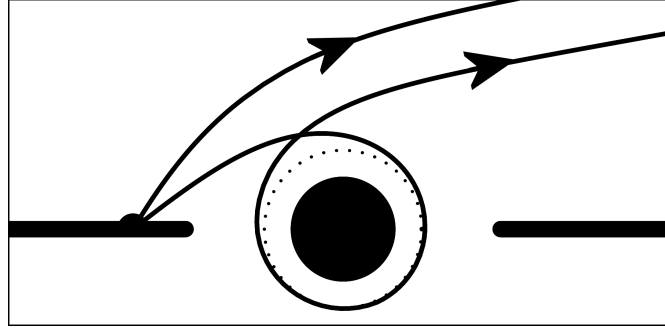


**Fig. 6** Trajectories of direct and looped photons emerging from a flare on the surface of an accretion disk. Figure reproduced from [61].

sponding to the travel time around the photon orbit and still with a sufficient intensity to be practically detected. If the delay in arrival time from the vicinity of a

**Table 1** Light circle timescales for different black hole sources: AGN, i.e. supermassive black holes in galactic centers, ULX i.e. hypothetical “intermediate mass” black holes postulated as an explanation of the Ultra Luminous X-ray sources, and GBH, i.e. microquasars in the Galactic black holes (X-ray binaries).

	Luminosity [erg/s]	Distance [kpc]	Timescale $T_{\text{photon}}$ [s]
AGN	$10^{41} - 10^{43}$	$10^3 - 10^4$	$10^2 - 10^4$
ULX	$10^{39} - 10^{41}$	$10^3 - 10^4$	$10^{-2} - 10^{-1}$
GBH	$10^{36} - 10^{38}$	$10^0 - 10^1$	$10^{-4} - 10^{-3}$

black hole between “direct” and “looped” photons could indeed be found in the light curves of AGNs or microquasars, it would not only provide an excellent tool to measure the mass and spin of the black hole, but it would also provide direct evidence for the existence of (nearly) circular photon orbits. In this way one would demonstrate the validity of an important prediction of general relativity in the regime of extremely strong gravitational field, see Table 1.

## 7 Conclusions

Today we have at hand strong observational arguments that, for all practical purposes, prove that the compact objects detected in the Galactic X-ray binaries and at the centers of our Galaxy, and other galaxies, are indeed black holes. We do not have yet similarly strong arguments, based on observational data, to prove that these are the Kerr black holes. Advanced instruments, planned for a near future, will provide

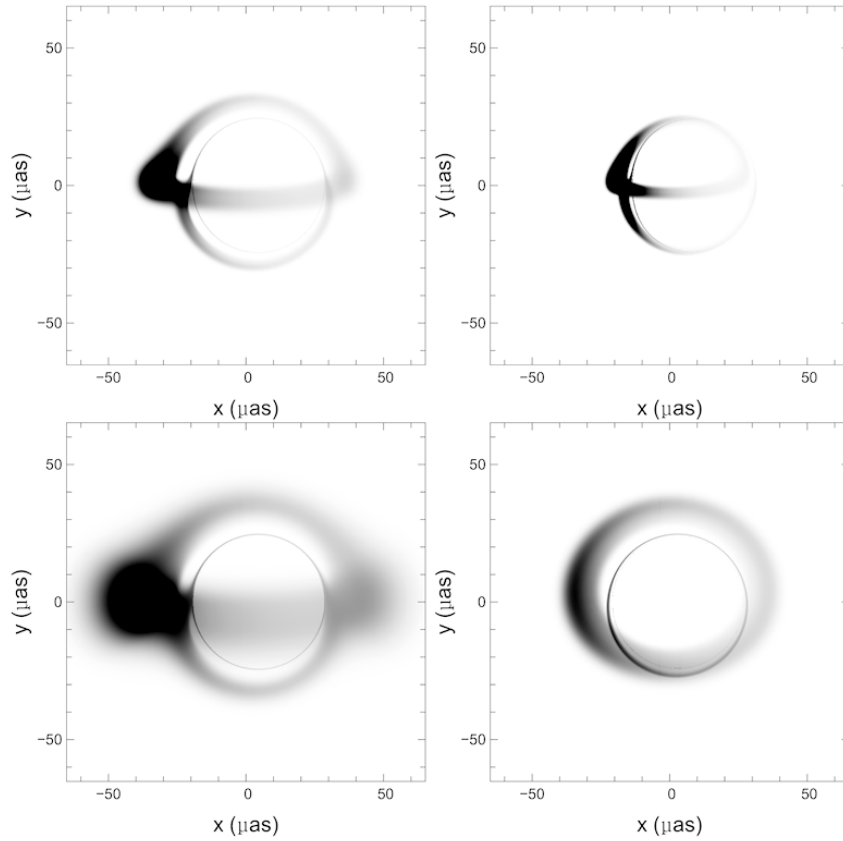


**Fig. 7** The circular light trajectory shows up in the theoretically calculated images of SgrA\*. Images taken from [62].

opportunities to probe the spacetime metric around the black hole candidates with a sufficient space (i.e. angular) and time resolution to obtain constraints.

**Acknowledgements:** My work at the Silesian University in Opava was supported by the Czech CZ.1.07/2.3.00/20.0071 “Synergy” grant for international collaboration, and at the Institute of Astronomy in Prague by the Czech ASCR M100031242 grant. I also acknowledge support from the Polish NCN grant UMO-2011/01/B/ST9/05439.

## References

1. K. Schwarzschild, *Über das Gravitationsfeld eines Massenpunktes nach der Einstein'schen Theorie*, Sitzungsberichte der Königlich Preussischen Akademie der Wissenschaften **1**, 189 (1916)
2. S. Chandrasekhar, *The maximum mass of ideal white dwarfs*, *Astrophys. J.* **74**, 81 (1931)
3. J.R. Oppenheimer, H. Snyder, *On continued gravitational contraction*, *Physical Review* **56**, 455 (1939)
4. M.A. Abramowicz, M. Jaroszyński, S. Kato, et al., *Leaving the innermost stable circular orbit: the inner edge of a black-hole accretion disk at various luminosities*, *A&A* **521**, A15 (2010)
5. R.P. Kerr, *Gravitational field of a spinning mass as an example of algebraically special metrics*, *Physical Review Letters* **11**, 237 (1963)
6. M. Dovciak, *Radiation of accretion discs in strong gravity*, ArXiv e-prints [arXiv:astro-ph/0411605] (2004)
7. M.R. Garcia, J.E. McClintock, R. Narayan, et al., *New evidence for black hole event horizons from Chandra*, *Astrophys. J. Letters* **553**, L47 (2001)
8. J.E. McClintock, R. Narayan, G.B. Rybicki, *On the lack of thermal emission from the quiescent black hole XTE J1118+480: Evidence for the event horizon*, *Astrophys. J.* **615**, 402 (2004)
9. R. Narayan, J.E. McClintock, *Advection-dominated accretion and the black hole event horizon*, *New Astr. Rev.* **51**, 733 (2008)
10. K. Menou, A.A. Esin, R. Narayan, et al., *Black hole and neutron star transients in quiescence*, *Astrophys. J.* **520**, 276 (1999)
11. R. Narayan, *George Darwin Lecture: Evidence for the black hole event horizon*, *Astronomy and Geophysics* **44**(6), 060000 (2003)
12. M.A. Abramowicz, W. Kluźniak, J.P. Lasota, *No observational proof of the black-hole event-horizon*, *A&A* **396**, L31 (2002)
13. J.P.S. Lemos, O.B. Zaslavskii, *Black hole mimickers: Regular versus singular behavior*, *Phys. Rev. D* **78**(2), 024040 (2008)
14. F. Yuan, E. Quataert, R. Narayan, *Nonthermal electrons in radiatively inefficient accretion flow models of Sagittarius A\**, *Astrophys. J.* **598**, 301 (2003)
15. A.E. Broderick, R. Narayan, *On the nature of the compact dark mass at the galactic center*, *Astrophys. J. Letters* **638**, L21 (2006)
16. R. Penrose, *Gravitational collapse: the role of general relativity*, *Nuovo Cimento Rivista Serie* **1**, 252 (1969)
17. R. Penrose, R.M. Floyd, *Extraction of rotational energy from a black hole*, *Nature Physical Science* **229**, 177 (1971)
18. J.M. Bardeen, W.H. Press, S.A. Teukolsky, *Rotating black holes: locally nonrotating frames, energy extraction, and scalar synchrotron radiation*, *Astrophys. J.* **178**, 347 (1972)
19. R.M. Wald, *Energy limits on the Penrose process*, *Astrophys. J.* **191**, 231 (1974)
20. A. Kovetz, T. Piran, *The efficiency of the Penrose process.*, *Nuovo Cimento Lettere* **12**, 39 (1975)
21. T. Piran, J. Shaham, *Upper bounds on collisional Penrose processes near rotating black-hole horizons*, *Phys. Rev. D* **16**, 1615 (1977)
22. R.M. Wald, *General relativity* (University of Chicago Press, 1984)
23. M. Bejger, T. Piran, M. Abramowicz, F. Håkanson, *Collisional Penrose process near the horizon of extreme Kerr black holes*, *Physical Review Letters* **109**(12), 121101 (2012)
24. M. Bañados, J. Silk, S.M. West, *Kerr black holes as particle accelerators to arbitrarily high energy*, *Physical Review Letters* **103**(11), 111102 (2009)
25. S.T. McWilliams, *Black holes are neither particle accelerators nor dark matter probes*, *Physical Review Letters* **110**(1), 011102 (2013)
26. A. Tchekhovskoy, R. Narayan, J.C. McKinney, *Black hole spin and the radio loud/quiet dichotomy of active galactic nuclei*, *Astrophys. J.* **711**, 50 (2010)

27. A. Tchekhovskoy, R. Narayan, J.C. McKinney, *Efficient generation of jets from magnetically arrested accretion on a rapidly spinning black hole*, Mon. Not. Roy. astr. Soc. **418**, L79 (2011)
28. J.C. McKinney, A. Tchekhovskoy, R.D. Blandford, *General relativistic magnetohydrodynamic simulations of magnetically choked accretion flows around black holes*, Mon. Not. Roy. astr. Soc. **423**, 3083 (2012)
29. R.D. Blandford, R.L. Znajek, *Electromagnetic extraction of energy from Kerr black holes*, Mon. Not. Roy. astr. Soc. **179**, 433 (1977)
30. R. Narayan, I.V. Igumenshchev, M.A. Abramowicz, *Magnetically arrested disk: an energetically efficient accretion flow*, Pub. Astr. Soc. Jap. **55**, L69 (2003)
31. B. Paczyński, *The inner boundary condition for a thin disk accreting into a black hole*, ArXiv e-prints [arXiv:astro-ph/0004129] (2000)
32. N. Afshordi, B. Paczyński, *Geometrically thin disk accreting into a black hole*, Astrophys. J. **592**, 354 (2003)
33. R. Shafee, J.E. McClintock, R. Narayan, et al., *Estimating the spin of stellar-mass black holes by spectral fitting of the X-ray continuum*, Astrophys. J. **636**, L113 (2006)
34. O. Straub, M. Bursa, A. Sądowski, et al., *Testing slim-disk models on the thermal spectra of LMC X-3*, A&A **533**, A67 (2011)
35. J.H. Krolik, *Magnetized accretion inside the marginally stable orbit around a black hole*, Astrophys. J. **515**, L73 (1999)
36. S.A. Balbus, *On the behaviour of the magnetorotational instability when the Rayleigh criterion is violated*, Mon. Not. Roy. astr. Soc. **423**, L50 (2012)
37. N.I. Shakura, R.A. Sunyaev, *Black holes in binary systems. Observational appearance.*, A&A **24**, 337 (1973)
38. I.D. Novikov, K.S. Thorne, *Astrophysics of black holes.*, in *Black Holes (Les Astres Occlus)*, ed. by C. Dewitt, B.S. Dewitt (1973), pp. 343–450
39. S.A. Balbus, J.F. Hawley, *A powerful local shear instability in weakly magnetized disks. I - Linear analysis. II - Nonlinear evolution*, Astrophys. J. **376**, 214 (1991)
40. O.M. Umurhan, K. Menou, O. Regev, *Weakly nonlinear analysis of the magnetorotational instability in a model channel flow*, Physical Review Letters **98**(3), 034501 (2007)
41. O. Regev, O.M. Umurhan, *On the viability of the shearing box approximation for numerical studies of MHD turbulence in accretion disks*, A&A **481**, 21 (2008)
42. S.A. Balbus, J.F. Hawley, *Instability, turbulence, and enhanced transport in accretion disks*, Reviews of Modern Physics **70**, 1 (1998)
43. S.A. Balbus, *Enhanced angular momentum transport in accretion disks*, Ann. Rev. Astr. Ap. **41**, 555 (2003)
44. B. Paczynski, G. Bisnovatyi-Kogan, *A model of a thin accretion disk around a black hole*, Acta Astr. **31**, 283 (1981)
45. B. Muchotrzeb, B. Paczynski, *Transonic accretion flow in a thin disk around a black hole*, Acta Astr. **32**, 1 (1982)
46. M.A. Abramowicz, B. Czerny, J.P. Lasota, E. Szuszkiewicz, *Slim accretion disks*, Astrophys. J. **332**, 646 (1988)
47. A. Sądowski, M. Abramowicz, M. Bursa, et al., *Relativistic slim disks with vertical structure*, A&A **527**, A17 (2011)
48. M.A. Abramowicz, W.H. Zurek, *Rotation-induced bistability of transonic accretion onto a black hole*, Astrophys. J. **246**, 314 (1981)
49. S. Hirose, O. Blaes, J.H. Krolik, *Turbulent stresses in local simulations of radiation-dominated accretion disks, and the possibility of the Lightman-Eardley instability*, Astrophys. J. **704**, 781 (2009)
50. S. Hirose, J.H. Krolik, O. Blaes, *Radiation-dominated disks are thermally stable*, Astrophys. J. **691**, 16 (2009)
51. R. Shafee, J.C. McKinney, R. Narayan, et al., *Three-dimensional simulations of magnetized thin accretion disks around black holes: stress in the plunging region*, Astrophys. J. **687**, L25 (2008)
52. C.S. Reynolds, A.C. Fabian, *Broad iron-K $\alpha$  emission lines as a diagnostic of black hole spin*, Astrophys. J. **675**, 1048 (2008)

53. R.F. Penna, J.C. McKinney, R. Narayan, et al., *Simulations of magnetized discs around black holes: effects of black hole spin, disc thickness and magnetic field geometry*, Mon. Not. Roy. astr. Soc. **408**, 752 (2010)
54. M. Abramowicz, A. Brandenburg, J.P. Lasota, *The dependence of the viscosity in accretion discs on the shear/vorticity ratio*, Mon. Not. Roy. astr. Soc. **281**, L21 (1996)
55. R.F. Penna, A. Sadowski, A.K. Kulkarni, R. Narayan, *The Shakura-Sunyaev viscosity prescription with variable  $\alpha(r)$* , ArXiv e-prints [[arXiv:1211.0526 \[astro-ph.HE\]](https://arxiv.org/abs/1211.0526)] (2012)
56. J.H. Krolik, J.F. Hawley, *Where is the inner edge of an accretion disk around a black hole?*, Astrophys. J. **573**, 754 (2002)
57. M.A. Abramowicz, W. Kluźniak, *A precise determination of black hole spin in GRO J1655-40*, A&A **374**, L19 (2001)
58. T.E. Strohmayer, *Discovery of a 450 HZ quasi-periodic oscillation from the microquasar GRO J1655-40 with the Rossi X-ray timing explorer*, Astrophys. J. Letters **552**, L49 (2001)
59. D. Barret, W. Kluźniak, J.F. Olive, S. Paltani, G.K. Skinner, *On the high coherence of kHz quasi-periodic oscillations*, Mon. Not. Roy. astr. Soc. **357**, 1288 (2005)
60. D. Barret, J.F. Olive, M.C. Miller, *Supporting evidence for the signature of the innermost stable circular orbit in Rossi X-ray data from 4U 1636-536*, Mon. Not. Roy. astr. Soc. **376**, 1139 (2007)
61. M. Bursa, M.A. Abramowicz, V. Karas, W. Kluźniak, A. Schwarzenberg-Czerny, *The timescale of encircling light*, in *Proceedings of RAGtime 8/9: Workshops on Black Holes and Neutron Stars*, ed. by S. Hledík, Z. Stuchlík (2007), pp. 21–25
62. O. Straub, F.H. Vincent, M.A. Abramowicz, E. Gourgoulhon, T. Paumard, *Modelling the black hole silhouette in Sagittarius A\* with ion tori*, A&A **543**, A83 (2012)